AQUEOUS ADULTERANTS REMOVAL BY PHOTOCATALYSIS CdO/CuO METAL OXIDE NANOCOMPOSITE

M. MAHENDIRAN[1], J. J. MATHEN[4], S. BHARATHI BERNADSHA[3], K. MOHAMED RACIK[2,3], J. MADHAVAN[3], M. JOE RAJA RUBAN [2,3], M. VICTOR ANTONY RAJ[2, 3*]

For innumerable purposes industries water is indispensable. In the recent days adulterants removal from the water is furthered by photocatalytic activity (PCA). The photocatalytic activity of CdO/CuO nanocomposite proposes it as a significant catalyst. The nanocomposite reacts with dye molecule and purifies the adulterants present in the contaminated water. Hydrothermal method is adapted to synthesize CdO/CuO nanocomposite. The synthesized CdO/CuO nanocomposite powder is characterized by XRD analysis. Photoluminescence spectra are useful data for revealing the trapping, relocation, and transfer of carriers. The enhancement of the PCA of the obtained catalyst is the focus of this work. The CdO/CuO nanocomposite gives the efficiency above 90 percent.

Keywords: CdO/CuO; Nanocatalyst; Contaminated water; Photocatalytic activity; Metal oxide;

1. Introduction

Safe and clean water providing system is an inevitable element of humanity's development and sustainability. The Photocatalytic Activity (PCA) attracts the researchers over the world, to reduce the colored organic dye present in the water. It is also useful to resolve the problem and to overcome the issues related to the energy and the environment [1]. The globe encounters pollution which affects environmental cycle especially water and air propelled by various pollution emitting industries [2]. At present, the effective elimination of several noxious residues from the drainages of the companies remains a big challenge. Dyes which are not ecofriendly but sold in market become contaminants.

The hazardous inorganic pollutants (phenols) like organic impurities (dyes and metal ions) are those elements present in wastewater [3, 4]. The different

[1] Department of Physics, DRBCCC Hindu College, Pattabiram, Chennai
[2] LIFE, Loyola College, Chennai, India.
[3] Department of Physics, Loyola College(University of Madras), Chennai, India.
[4] Department of Physics, St. Thomas College, Palai, Kerala, India
Corresponding author: vicvad2003@yahoo.co.in*

potential organic pollutant elements are Methyl Orange, Rhodamine B, Methylene Blue and Orange II diazo inorganic pollutants which are to be removed or reduced. Methyl Orange is emerging contaminants organic in nature, which is mostly used as a dye material [5, 6]. The uncontaminated habitat and freshwater body is needed for the health of the humanity and living beings in water. Hence, the elimination of organic contaminants from wastewater is necessary for a conducive environment. The eradication of dye molecule from the contaminant water involves the breaking of complete conjugated unsaturated bonds in molecule. The photocatalytic activity (PCA) degrades the dye contents through decolorization or decontamination from the contaminant water. Thus it is demonstrated to be the excellent increasing efficient method. The nanocomposite has an incomparable role to play in heterogeneous catalysis and it produces harmless materials from the dangerous pollutants.

2. Materials and Method

The CdO/CuO nanocomposite is synthesized by a facile and trouble-free, hydrothermal method. For this, 0.2M of Cd $(CH_3COO)_2x2.H_2O$ (Cadmium acetate dihydrate) and 0.76g of Copper Acetate Dihydrate (Cu $(CH_3COO)_2x2.H_2O$) are mixed in 70mL water which is deionized 0.5g sodium hydroxide was mixed with double refined water of 20mL and it is then mingled in drops to the solution under continuous stirring for 30 min. The contents of the perfect solution is then shifted to an autoclave and placed in an oven at 140° C for 12h. Through the gradual cooling process, the solution reaches its normal temperature. Using water that is doubly deionized and ethanol the commodity attained is washed five times and it is dried at 80° C for 12 (twelve) hours. The white powder stranded at the base is collected and annealed at 500° C for 3hours. Eventually, black colored nanocomposite of CdO/CuO nanoparticles is successfully obtained.

3. Results

3.1 Size and Strain Analysis

To find the purity of the crystalline phases of CdO/CuO nanocomposite X-ray diffraction (XRD) measurement results are plotted in Fig. 1. The obtained peaks in XRD results can be attributed to the cubic phase of CdO (cadmium oxide) (JCPDS card no: 05-0640) monoclinic phase of CuO (copper oxide) (JCPDS NO. 36-1451). The XRD crests of the CdO/CuO nanocomposite reveals that the relatively strong diffraction symbolizes CdO/CuO nanostructures possess good crystallinity. Surprisingly, impurity is not identified in the X-ray diffraction pattern. The XRD pattern of CdO/CuO shows a sequence of high and low intensity peaks. The Scherrer's equation measure the crystal size (average) as:

$$D = \frac{k\lambda}{\beta cos\theta} \quad (1)$$

D - average crystallites size; K-shape factor (0.94); β – FWHM; θ -Bragg's angle; wavelength of X-ray λ=1.54Å. 41nm is the determined average crystallite size of CdO/CuO nanocomposite. Williamson–Hall analysis is simplified into integral breadth method that differentiates size, strain induced crests broadening by considering the crests width as 2θ function. According to study of this W-H exploration the crest width at half maximum intensity (β_{hkl}) is a function of crystallites size and the lattice strain equation [7];

$$\beta_{hkl} = \beta_{crytallite} + \beta_{strain} \quad (2)$$

The broadening accredited to lattice strain in the powders is calculated using equation (3)

$$\beta_{strain} = 4\varepsilon \tan\theta \quad (3)$$

Rearranging the equation (2) gives

$$\beta_{hkl} Cos\,\theta = \frac{k\lambda}{D} + 4\varepsilon \sin\theta \quad (4)$$

Fig. 2 exhibits the linear fit curve of 4 sin θ vs β_{hkl}cosθ. Average size (crystal) and dislocation are calculated in the extrapolation and slope obtained as 43 nm and 0.0031 respectively. Thus, mean size of the crystals is determined by W-H method in line with the result obtained in Scherrer's method.

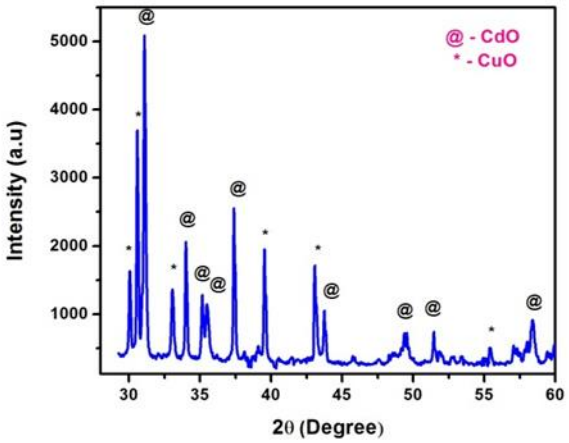

Fig. 1: X-Ray Diffraction of nanocomposite CdO/CuO

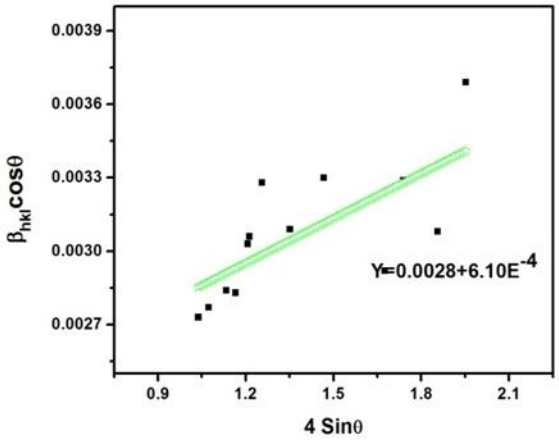

Fig. 2: W-H plot of nanocomposite CdO/CuO

3.2 Morphology Analysis

The HR-SEM, HR-TEM images EDAX and spectrum SAED of CdO/CuO nanocomposite are plotted in Fig. 3 (a, b, c and d). HR-SEM reveals the individual spherical Nano flake with a high compact structure. The structure could improve the photocatalytic (PC) properties by easing the charge carrier's transport. The obtained average diametrical size is about 35-55 nm. HR-SEM results and Scherrer formula, Williamson-Hall plot method confirms the particle size achieved from. The EDAX analysis exposes that the elements of CdO/CuO nanocomposite are present in the synthesized powder sample. The major elements present are cadmium Cd (76.16 wt%), copper Cu (12.35wt%) and oxygen O (11.49 wt%). EDAX spectrum is free of unwanted peaks which confirm that the composite sample is impurity absent. TEM analysis and SAED pattern clearly exhibit that a spherical rod is formed and concentric rings match well with CdO/CuO nanocomposite.

3.3 Optical Studies

Fig. 4 indicates the UV-Vis spectrum of CdO/CuO nanocomposites. This shows a maximum absorption crest at 327 nm which is a violet shift in the electromagnetic region. E_g is obtained from Tauc plot (Fig. 5).

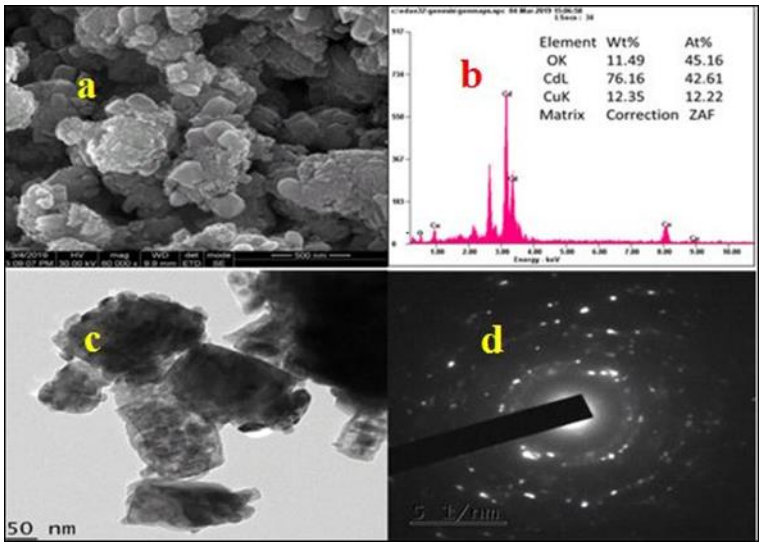

Fig. 3: Images of a) HRSEM, b) TEM, c) EDAX and d) SAED pattern of nanocomposite CdO/CuO

Based on direct allowed transition type, the optical energy band gap of the sample was found using Tauc's relation [14].Tauc plot graph is drawn with energy (hv) against $((\alpha hv)^2$ in Fig. 5. Deducing the linear portion of the contour to zero absorption, the E_g of 3.72 eV is obtained. Excitation of electrons are speeded up by the decrease of energy band gap (between VB and CB) exploiting low energy which will make available more electron hole pairs and improve the removal of the dyes through PC activities.

3.4 Photoluminescence Analysis

Photoluminescence spectra reveal the relocation, trapping, and exchange of electron carriers. PL emission is highly dependent on the re-combination of free carriers (Fig. 6) [15]. The emission crest at 420 nm has been ascribed to the changeover between defects (interface traps) at grain boundaries and the valence bands lattice defects that are related to vacancy of oxygen [19-21]. The green emission crest at 529 nm rises due to recombination of photo-generated hole (h^+) and singly ionized oxygen. The spectra consist of an acute and strong emission band at 486 nm. The near band-edge narrow UV crest located at 408 nm can be attributed to direct radiative recombination of excitons and the UV-visible crest at 420 nm and 446 nm appeared as a result of charge carrier relaxation.

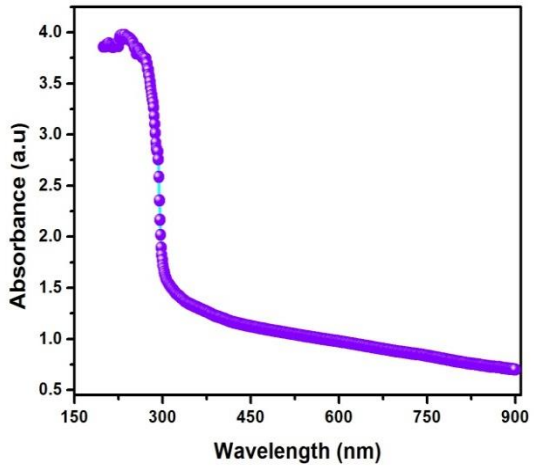

Fig..4: UV-Visible Spectrum of CdO/CuO

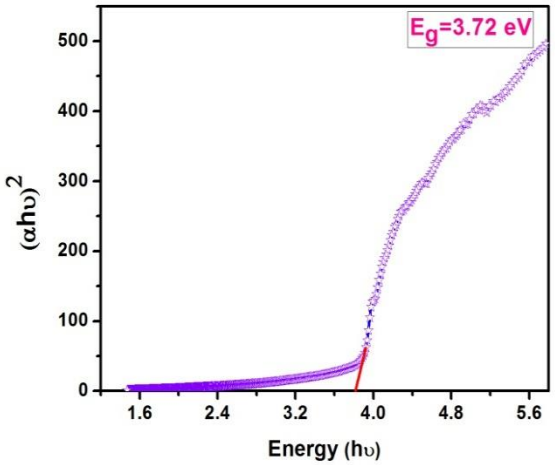

Fig. 5: Tauc Plot of CdO/CuO

It happens due to the occurrence of surface related trap states. In case of excitonic PL signals, the lower peak intensity shows the reduction of charge carrier recombination. There is a high possibility for diminishing of peak intensities due to the presences of very small CuO content in CdO nano flake sample, by charge carrier separation, can largely suppress photo-induced electron-hole recombination [22].

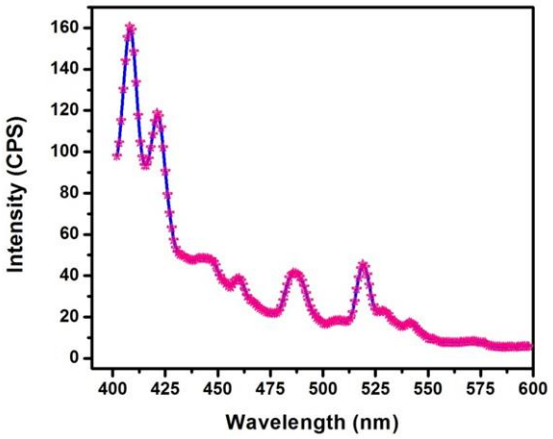

Fig. 6: Photoluminescence (PL) spectrum of nanocomposite CdO/CuO

3.5. Measurement of Photocatalytic Activity (PCA)

Fig. 7 shows the experiment of PCA. Methyl orange organic dye is taken for the study of PCA of the synthesized sample. To prepare contaminated water, methyl orange dye is taken as 0.001g and deliquesces in deionized prepared solution is dissolved in catalyst of 0.1g and this mixture is kept in a tightly closed dark room and uniformly stirred for 30 min using magnetic stirrer. After 15 min the solution is kept under the ultraviolet light source (100W mercury lamp) and the suspension was continuously stirred manually. At the interval of 5 min the irradiated solution is removed from the suspension. The complete decolorization is observed at 75 min. The absorption spectrum of the cleared solution is recorded. The collected sample solutions are characterized by UV studies. Degradation extent is determined in terms of the changes in intensity at the λ_{max}= 462nm for methyl orange.

The decolorization range is estimated by the equation (5).

$$\text{Percentage of Methyl Orange Degradation} = \frac{Ci - Cf}{Ci} \times 100 \quad (5)$$

Where, C_i is the initial concentration absorption of each dye, C_f is the final concentration absorption of each dye.

Fig. 8 illustrates the wavelength vs absorbance of CdO/CuO nanocomposite. The crystalline size, morphology, optical energy gap increase the absorption strength and superior partition of photogenerated electron-hole pairs. Hence, photocatalytic (PC) achievement also enriched (Fig. 9).

This result confirms the contriving mechanism of the methyl orange (MO) degradation process on the surface of the CdO/CuO nanocomposite. Semiconductor nanocomposite is formed by the combination of two metal oxides

which have properly selected values for electronic band potential. The mixed nanocomposite consists of two main semiconductors, one is CdO with an energy band gap of 2.5 eV and other is 1.7eV. The Semiconductor nanocomposite copper oxide has a band gap which is very narrow. This narrow band gap shifts the absorption band along the visible light direction and also separates photogenerated electron-hole (e^-+h^+) charge carriers, thus slowing recombination. Zinc oxide and copper oxide are applied over the surface which paves way in increased contact surface of the catalyst with dye nanoparticles, resulting in oxygen diffusion and transport of dye in mass quantity photochemical reaction. The modification of zinc oxide with the addition of copper oxide (CdO) increases the wavelength (λ) range which increases the efficiency of energy used in the visible light range. The CdO/CuO hetero structure helps in separation of generated electron-hole (e^-+h^+) pairs in the presence of photon. Electrons (e^-) move from valence band to conduction band while leaving holes positive (h^+). Because Copper oxide holds (CuO) a higher energy band to zinc oxide (ZnO) band and hence conduction band and valence bands lie above in CuO (which thermodynamically promote the exchange and transfer of excited electrons and holes between them), this behavior results in increased ZnO quantum efficiency which is the result of separation of carriers in different semiconductors, effectively inhibiting the recombination of electron-hole (e^-+h^+) pairs. After the separation of electrons (e^-) and holes (h^+), reactions of formation of hydroxyl radicals (OH^-) occur, which react with organic or contaminate substances in water (H_2O) that can be degraded to CO_2 and H_2O.

The reaction of photocatalytic mechanism involves a few steps like ionization of water, light excitation, absorption of oxygen ion and superoxide protonation. When a photon is subjected to illuminate a metal photo catalyst it will create an electron hole pairs. At the surface of photon or light got excited photocatalyst reduction and oxidation takes place. Then the catalyst particle absorbs photon and creates a positive charged h^+ reacts with H_2O molecule to produce radicals. Catalysis reacts with dissolved oxygen to generate $O_2\bullet^-$ radical ions that are able to degrade methyl orange (MO). Photogenerated electrons (e^-) can react with molecular oxygen (O) to formless noxious superoxide anion ($*O_2^-$) radicals through a minimal process whereas the h^+ reacts with H_2O or hydroxyl ions (OH^-) to form the most reactive hydroxyl (*OH) radicals through the oxidative process. The electron–hole pairs react with superoxide anions to generate hydrogen peroxide (H_2O_2). The one metal oxide combine with another metal oxide has produced more dynamic photocatalytic centre which assist the photocatalytic degradation performance.

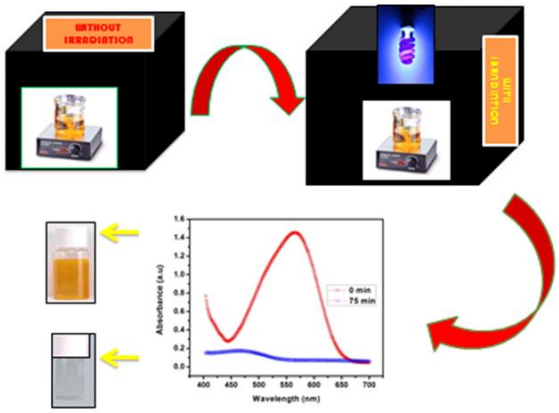

Fig. 7: Schematic diagram of photocatalytic experiment

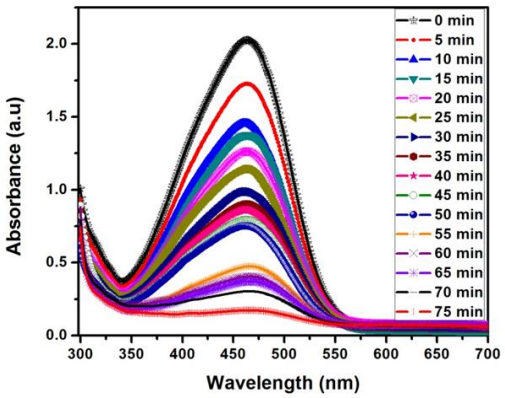

Fig. 8: Absorption graph of CdO/CuO nanocomposite

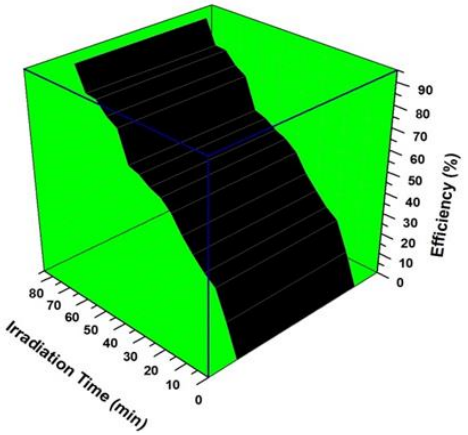

Fig. 9: Decolorization efficiency of CdO/CuO nanocomposite

4. Conclusion

The quality of the crystallite CdO/CuO nanocomposite plays the major role in removing the adulterant from the water. Removing adulterant from the water will make clean environment. The crystal size and morphology of catalyst is examined by X-ray Diffraction HR-SEM and TEM analysis. The nanocomposite's crystallite size is 41nm determined using X-ray diffraction analysis. HR-SEM and TEM studies show the morphology as rod spherical and rod flake respectively. Band gap of the composite are found by UV-Vis spectrometer. The band gap of the nanocomposite has been found as 3.72eV.PL analysis gives the defects of the crystallite. This combination gives favorable PCA performance which is 90%. This promises the obtained composite is suitable for removing the adulterant from the water.

R E F E R E N C E S

[1]. *C. G. Tian, Q. Zhang, A. P. Wu, M. J. Jiang, Z. L. Liang, B. J. Jiang and H. G. Fu*, "Environmental Photocatalysis" in Chem. Commun. **vol 48 ,**no 23, Nov2012, pp2858–2860.

[2]. *C. Tongqin, L. Zijiong, Y. Gaoqian, J. Yong, Y. Hongjun*, "Enhanced photocatalytic activity of ZnO/CuO nanocomposites synthesized by hydrothermal method." in Nano-Micro Lett., **vol 5,** Sep 2013, pp 163–168.

[3]. *S.Siuleiman, N. Kaneva, A. Bojinova, K. Papazova, A. Apostolov, D. Dimitrov*, "Photodegradation of Orange II by ZnO and TiO2 powders and nanowire ZnO and ZnO/TiO2 thin films." in Colloids and Surfaces A: Physicochem. Eng. Aspects, **vol 460**,Oct 2014, pp 408-413.

[4]. *Devan RS, Patil RA, Lin JH, Ma YR.*, "One-Dimensional Metal-Oxide Nanostructures: Recent Developments in Synthesis, Characterization, and Applications" inAdv Funct Mater **vol 22**, no 33,Jun 2012, pp 26-70.

[5]. *Wang G, Ling Y, Li Y*, "Graphene-Based Glucose Sensors: A Brief Review" Nanoscale **vol 4** no 66, Nov 2012,pp82-91.

[6]. Y*ang, Lixia, Z Li, H Jiang, W Jiang, R Su, S Luo, and Y Luo.*"Photoelectrocatalytic oxidation of bisphenol A over mesh of TiO_2/graphene/Cu_2O." in Applied Catalysis B: Environmental **vol 183**,Apr 2016, pp75-85.

[7]. *Z, J.; Hu, Y.; Jiang, X.; Chen, S.; Meng, S.; Fu, X.* "Design of a direct Z-scheme photocatalyst: preparation and characterization of Bi2O3/g-C3N4 with high visible light activity." in J. Hazard. Mater. **vol 280**, Sep 2014, pp 713-722.

[8]. *M. Mahendiran, J.J. Mathen, Mohamed Racik, J. Madhavan, M. VA Raj* "Investigation of structural, optical and electrical properties of transition metal oxide semiconductor CdOZnO nanocomposite and its effective role in the removal of water contaminants." in J. of Phy and Chem of Solids, **vol 126**, Mar 2019,pp 322-334.

[9]. *S. Harish J. Archana M. Sabarinathan M. Navaneethan K.D. Nisha S. Ponnusamy C.*

Muthamizhchelvan H. Ikeda D.K. Aswal Y. Hayakawa "Controlled structural and compositional characteristic of visible light active ZnO/CuO photocatalyst for the degradation of organic pollutant." in Applied Surface Science **vol 418**, Part A, no 1 October 2017, pp 103-112.

[10]. *Anand, A. Persis Amaliya, M. AsisiJanifer, S. Pauline* "Structural, morphological and dielectric studies of zirconium substituted CoFe2O4 nanoparticles." in Modern Electronic Materials Dec 2017, pp 168–173.

[11]. *R.M. Mohamed, F.A. Harraz, A. Shawky,* "CuO nanobelts synthesized by a template-free hydrothermal approach with optical and magnetic characteristics." in Ceram. Int. **vol 40** Jan 2014,pp 2127-2133.

[12]. *Sneha G. P, J P. Corbett, M Wojciech. Jadwisienczak, E Martin. Kordesch* "Structural characterization and X-ray analysis by Williamson–Hall method for Erbium doped Aluminum Nitride nanoparticles, synthesized using inert gas condensation technique." in Physica E: Low-dimensional Systems and Nanostructures **Vol 79,** May 2016, pp 98-102.

[13]. *S. Sumithra, N.V. Jaya,* "Band gap tuning and room temperature ferromagnetism in Co doped Zinc stannate nanostructures." in Physica B **vol 493,** Jul 2016, pp 35-42.

[14]. *S.D. Tiwari, K.P. Rajeev,* "Signatures of spin-glass freezing in NiO nanoparticles." in Phys. Rev. B , **vol 72,** Sep 2005, pp 104433.

[15]. *H. Li, L. Zhu, M. Xia, N. Jin, K. Luo, Y. Xie,* "Synthesis and investigation of novel ZnO–CuO core-shell nanospheres." in Mater. Lett. **vol 174,** Jul 2016, pp 99-101.

[16]. *J.Y. Yu, S.D. Zhuang, X.Y. Xu, W.C. Zhu, B. Feng, J.G. Hu,* "Photogenerated electron reservoir in hetero-p–n CuO–ZnO nanocomposite device for visible-light-driven photocatalytic reduction of aqueous Cr (VI)." in J. Mater. Chem. A **vol 3,** 2015, pp 1199.

[17]. *P. Lu, W. Zhou, Y. Li, J. Wang, P. Wu,* "Abnormal room temperature ferromagnetism in CuO/ZnO nanocomposites via hydrothermal method." in Appl. Surf. Sci. **vol 399,** Mar 2017,pp 396-402.

[18]. *Ashar A, Iqbal M, Bhatti IA, Ahmad MZ, Qureshi K, Nisar J, et al*. . "Hydrothermal synthesis of molybdenum trioxide, characterization and photocatalytic activity." in J Alloy Comp **vol 678,** feb 2016,pp126-36.

[19]. *Yang, C. Cao, X. Wang, S. Zhang, L. Xiao, F. Su, X. Wang,* . "Complex-directed hybridization of CuO/ZnO nanostructures and their gas sensing and photocatalytic properties." in J. Ceram Int. **vol 41,** Jan 2015, pp1749-1756.

[20]. *Sahay, Sundaramurthy R, J. Kumar, Thavasi P. S., Mhaisalkar V, S. G. Ramakrishna, S.* . "Synthesis and characterization of CuO nanofibers, and investigation for its suitability as blocking layer in ZnO NPs based dye sensitized solar cell and as photocatalyst in organic dye degradation." in J. Solid State Chem. **vol 186,** Feb 2012,pp 261-267.

[21]. *Yang, X.; Shao, C. Guan, H. Li, X. Gong,* "Novel nanocomposites and nanoceramics based on polymer nanofibers using electrospinning process—a review." in the J. Inorganic. Chem. Commun. **vol 7,** Aug 2004, pp 176-178.

[22]. *Samadi, M.; Shivaee, H. A.; Zanetti, M.; Pourjavadi, A.; Moshfegh,,*"Visible light photocatalytic activity of novel MWCNT-doped ZnO electrospun nanofibers." in the J. Mol. Catal.A: Chem. **vol 359,** Jul 2012, pp 42-48.